

Dream fusion in octahedral spherical hohlraum



Cite as: Matter Radiat. Extremes 7, 055701 (2022); doi: 10.1063/5.0103362
Submitted: 15 June 2022 • Accepted: 11 August 2022 •
Published Online: 8 September 2022



Ke Lan^{a)}

AFFILIATIONS

Institute of Applied Physics and Computational Mathematics, Beijing 100094, China and HEDPS, Center for Applied Physics and Technology, and College of Engineering, Peking University, Beijing 100871, China

^{a)} Author to whom correspondence should be addressed: lan_ke@iapcm.ac.cn

ABSTRACT

The octahedral spherical hohlraum provides an ideal and practical approach for indirect-drive toward a dream fusion with predictable and reproducible gain and opens a route to the development of a laser drive system for multiple laser fusion schemes. This paper addresses a number of issues that have arisen with regard to octahedral spherical hohlraums, such as how to naturally generate a highly symmetric radiation drive at all times and for all spectra without the use of symmetry tuning technology, how to determine the three-dimensional, temporal, and spectral characteristics of the real radiation drive on a capsule in experiments, and the relative energy efficiency of an octahedral spherical hohlraum compared with a cylindrical hohlraum. A design island for an octahedral spherical hohlraum is presented. Finally, the challenges and future tasks for the path forward are presented.

© 2022 Author(s). All article content, except where otherwise noted, is licensed under a Creative Commons Attribution (CC BY) license (<http://creativecommons.org/licenses/by/4.0/>). <https://doi.org/10.1063/5.0103362>

I. INTRODUCTION

Energy from controlled nuclear fusion has been a quest of scientists worldwide for more than a half a century,^{1–3} and achieving a predictable and reproducible fusion gain is the first step toward an inertial fusion energy power plant. In indirect-drive inertial fusion, a spherical encapsulated deuterium–tritium (DT) fuel pellet of millimeter-size is irradiated and imploded with a very high velocity by x-rays converted from lasers inside a centimeter-size hohlraum, thereby compressing it to extreme density, temperature, and pressure to release significant fusion energy. The world's largest laser facility, the National Ignition Facility (NIF),^{4–6} the size of three football fields, aims to achieve fusion ignition via an indirect-drive scheme. Recent striking progress on the NIF, with 1.37 MJ fusion yield^{7–10} for ~70% of the input laser energy, has come close to demonstrating the feasibility of the indirect drive for clean and sustainable energy production. However, it should be recognized that this remarkable achievement of the NIF has been the culmination of many years of experiments and simulations, including symmetry tuning campaigns,^{10–15} determinations of the appropriate level of irradiation of the capsule from implosion performance,^{6,16} investigations of the effects on the incidence angle of the laser pulse and the use of time-dependent multipliers,^{10,17,18} and iterations to find the right design parameters to produce the required spherical radiation

drive inside cylindrical hohlraums.^{10,15,19} Note that the symmetry tuning techniques used on the NIF are aimed mainly at suppressing the Legendre polynomials P_2 , which represent the inherent asymmetry of all kinds of hohlraums with two laser entrance holes (LEHs). It is clear that the NIF will meet even greater challenges on the road to achieving a predictable and reproducible fusion at high gain. Nevertheless, its historic achievement and lessons provide clues to enable further progress to be made toward a dream fusion at an upgraded facility with simple and robust target designs.

To achieve a dream fusion expected from an ideal design of a high-convergence spherical implosion, with predictable and reproducible ignition and gain, there are three prerequisites: (1) a credible one-dimensional (1D) theoretical design of a spherical implosion at a convergence ratio higher than 30, (2) sufficient laser energy to irradiate the hohlraum and generate an implosion producing the required radiation energy, and (3) a highly symmetric spherical radiation drive with the implosion required temporal and spectral characteristics. With regard to the first of these, a near-1D indirectly driven implosion has been successfully achieved at a convergence ratio 30 on the NIF, thus demonstrating the credibility of 1D implosion design at such a high convergence ratio.²⁰ With regard to the second prerequisite, a systematic analysis of the hohlraum energetics experiments has shown that the NIF energy is sufficiently high to generate the radiation energy required

for ignition.²¹ However, it is unfortunately not easy to fulfill the third prerequisite and create spherically symmetric radiation on the NIF.

As is well known, the major obstacles preventing ignition at the NIF include asymmetry of target irradiation, laser plasma instabilities (LPIs), and hydrodynamic instabilities.^{22–24} However, viewed from another angle, leaving engineering issues aside, the relevant problems are completely physical issues concerning the radiation drive. To achieve the dream fusion expected from an ideal design of high-convergence spherical implosion, an ideal and clear radiation drive is necessary. In other words, it is hard to achieve a dream



FIG. 1. Dream fusion in an octahedral spherical hohlraum. An octahedral hohlraum has six LEHs of the same size, with one at each pole and four along the equator, injected with lasers in an ideal arrangement. For the sake of illustration, as shown in Fig. 2, we number the LEHs centered on the positive and negative z axes (denoted by $+z$ and $-z$) as I and VI, respectively, those on $+x$ and $-x$ as II and IV, respectively, and those on $+y$ and $-y$ as III and V, respectively. The laser beams are clustered in quads, characterized by the incidence angle θ_L formed with the respective LEH axis and the azimuthal angle ϕ_L around that axis. In the ideal laser arrangement, all LEHs have the same quad number N_Q , all quads have the same θ_L ranging from 50° to 60° , and the quads of each LEH are aligned evenly in azimuth at $\phi_L = \phi_{L0} + k \times 360^\circ / N_Q$ ($k = 1, \dots, N_Q$) with $0^\circ < \phi_{L0} < \phi_{LM}$ and $\phi_{LM} = 360^\circ / 2N_Q$. Here, ϕ_{L0} is the initial azimuthal angle deviating from $+x$ and $-x$ in the xy plane for LEH I and VI, respectively, from $+y$ and $-y$ in the yz plane for II and IV, respectively, and from $+z$ and $-z$ in the zx plane for III and V, respectively. Cylindrical LEHs are used to improve the laser beam propagation inside the spherical hohlraum. Also, the use of LEH shields can be considered, with the aim of decreasing radiation loss via the six LEHs and increasing the radiation asymmetry.

fusion with a nonideal and unclear drive. An ideal drive must meet two requirements: (1) it must remain highly symmetric at all times and for all spectra; (2) it must have all the required characteristics with regard to time and spectrum. Thus, it is necessary to understand the real drives that are used in experiments and know how far away they are from what is to be expected to be needed for successful ignition. Two questions then arise: First, how can the desired highly symmetric radiation drive be generated at all times and for all spectra? Second, what are the three-dimensional (3D), temporal, and spectral characteristics of the radiation drives in real experiments? The solutions are strongly connected with the approach of hohlraum configuration and laser arrangement.

For many decades, the mainstream approach has been based on hohlraums with cylindrical symmetry,² such as the NIF, and the Laser Mega-Joule (LMJ)²⁵ and the SG series²⁶ laser facilities, all of which need supplementary technology to tune and create a spherical radiation drive inside hohlraums with two LEHs. However, it is hard to tune to obtain highly symmetric radiation at all times and for all spectra, let alone with the characteristics required by ignition capsules. Furthermore, the tuning itself is complicated and even unpredictable, which makes the radiation source more uncontrollable and unpredictable, further aggravating the problem.

As shown in Fig. 1, we proposed an octahedral spherical hohlraum^{27–30} (hereinafter referred to simply as an octahedral hohlraum) in 2013 and have studied it for nearly a decade both theoretically and experimentally on the SG laser facilities. From our studies, we have found that the octahedral hohlraum is an attractive concept for the next generation of laser systems, with the merits that it provides an ideal answer to the two questions raised above and a practical way toward dream fusion. The octahedral hohlraum campaign started in 2014, including demonstrations of improved laser propagation inside spherical hohlraums by using cylindrical LEHs,^{30–33} hohlraum energetics,^{34–36} comparisons of LPI between spherical and cylindrical hohlraums and a demonstration of low LPI with an octahedral hohlraum design,^{37,38} and a proof-of-concept experiment.³⁹ The campaign has successfully demonstrated the key designs and proof of concept of the octahedral hohlraum and has attracted broad interest from the fusion community.^{40–55}

II. HOW CAN SPHERICAL RADIATION BE GENERATED INSIDE A OCTAHEDRAL HOHLRAUM AT ALL TIMES AND FOR ALL SPECTRA? WHAT IS THE IDEAL LASER ARRANGEMENT?

The laser arrangement is key to retaining the high symmetry of an octahedral hohlraum. The ideal laser arrangement design of an octahedral hohlraum²⁸ is presented in Fig. 1, which results from a comprehensive consideration of radiation symmetry, energy coupling efficiency, LPI, and hydrodynamic instabilities. Without any supplementary technology for symmetry tuning, it can naturally convert 3D lasers into quasi-1D spherical radiation. From our 3D view factor code VF3D, at a hohlraum-to-capsule radius ratio larger than 3.7, we find that the asymmetry of the octahedral hohlraum can be lower than 1%^{28,56} without any symmetry tuning technology, easily meeting the ignition requirement.^{2,57} This ideal laser arrangement provides the following enormous advantages.

First, the ideal laser arrangement perfectly retains the high symmetry of a 6-LEH spherical hohlraum and can naturally and robustly

create highly symmetric radiation inside the hohlraum at all times and for all spectra. Relative to the six LEHs, the laser spots look like numerous stars dressing the hohlraum around the sky.^{29,56} Hence, the radiation asymmetry is determined mainly by the two geometrical ratios of the target, i.e., the hohlraum-to-capsule radius ratio and the LEH-to-capsule radius ratio, while the contribution from the laser can be neglected.^{28,56} As a result, the symmetry is robust and insensitive to laser power imbalance, laser pointing accuracy, and accuracy of assembly.^{28,56,58} Under this ideal laser arrangement, the radiation distribution does not contain asymmetries corresponding to the spherical harmonic modes $l = 2$ and all odd l , and the asymmetry corresponding to $l = 6$ is at a very low level. Choosing the golden hohlraum-to-capsule radius ratio²⁸ of around 5, the mode $l = 4$ is completely suppressed, leaving $l = 8$ as the dominant mode.

Second, all laser quads inside the octahedral hohlraum are the same, with no laser crossing inside the hohlraum, no overlapping of laser spots on the hohlraum wall, and no interplay between laser propagation and ablated material from the capsule. This is very different from the case of the cylindrical hohlraums of the NIF.^{59–61} As a result, there is no need to tune the symmetry via nonlinear cross-beam energy transfer, no need to adjust different temporal pulse shapes among beams with different injection angles, and no need to suppress the serious laser plasma instabilities of laser beams at small injection angles, resulting in more efficient energy coupling and significant suppression of potentially dangerous nonlinear processes. Furthermore, the relatively simple and clean environment makes it possible to find a physical solution that enables determination of the actual radiation drive on the capsule inside an octahedral hohlraum.

Third, the ideal laser arrangement of an octahedral hohlraum can be applied to diverse fusion schemes,^{28,29,52,56} such as indirect drive,² direct drive,⁶² hybrid-drive,⁶³ and laser-driven spherically convergent plasma fusion.^{64,65} Note that the octahedral laser arrangement keeps all laser quads the same, and hence it can also retain symmetry for all nonlinear phenomena associated with LPI inside a spherical hohlraum for indirect drive.²⁸ For direct drive, a high degree of uniformity in laser energy deposition on the capsule targets is also required,^{51,52,66–68} and this can be achieved by using this ideal laser arrangement via laser shifting within the adjustments permitted by laser engineering. Indeed, the octahedral hohlraum represents an enormous advance for all indirect-drive or direct-drive based approaches, which need a spherical drive for spherical implosions. Thus, the ideal laser arrangement opens the way to a drive laser system applicable to multiple schemes.

III. WHAT ARE THE 3D, TEMPORAL, AND SPECTRAL CHARACTERISTICS OF REAL RADIATION DRIVES? CHARACTERISTIC REGIONS

Only by determining the real drive felt by the capsule in an experiment can we know how far away it is from the design and then accurately adjust it to meet requirements. Even for postshot simulations of hydrodynamic instability,⁶⁹ which is one of the major obstacles preventing ignition at the NIF, the real radiation drive is needed as an input. However, since the beginning of indirect-drive experiments, it has been a puzzle to accurately determine the

actual characteristics of the radiation on the capsule.^{70,71} First, it is hard to directly measure the radiation on such a small capsule of 2–3 mm inside a hohlraum 1 cm in size. Second, it is usual to measure the radiation flux streaming out of an LEH and then take the result at a single angle as the radiation drive.^{2,57,70} However, owing to the limited field of view, the presence of cold plasma outside the hohlraum, and shrinking of the LEH, it is hard to find an angle at which the observed radiation at all times and for the full spectrum is the same as that seen by a capsule located at the center of the hohlraum here, let alone that the radiation distribution on capsule is actually 3D. Third, the ViewFactor method was proposed to characterize the capsule x-ray drive,⁷² but it needs an open geometry, which has a deleterious effect on the hohlraum radiation environment. Fourth, the witness method also changes the radiation drive on the capsule by placing a witness plate inside the hohlraum.^{2,36,57,70,73} Thus, up to now, the real radiation drives of the NIF hohlraums have not been entirely clear. In fact, owing to the very complicated environment inside a cylindrical hohlraum, it is hard to know the 3D, temporal, and spectral characteristics of the real radiation drive.

However, benefiting from the simple and clean hohlraum environment inside an octahedral hohlraum, there is a physical solution to the real drive problem. Inside an octahedral hohlraum, the radiation on the capsule is contributed mainly by the characteristic regions, including the hot laser spots, the cool re-emitting wall, and the cooler closing LEHs, as shown in Fig. 2. Hence, we can determine the radiation drive in the following way. First, we measure the temporal and spectral emissions of all kinds of characteristic regions using diagnostics outside the LEHs. Second, by putting the measured data into an extended view factor model,^{28,74} we can reconstruct the

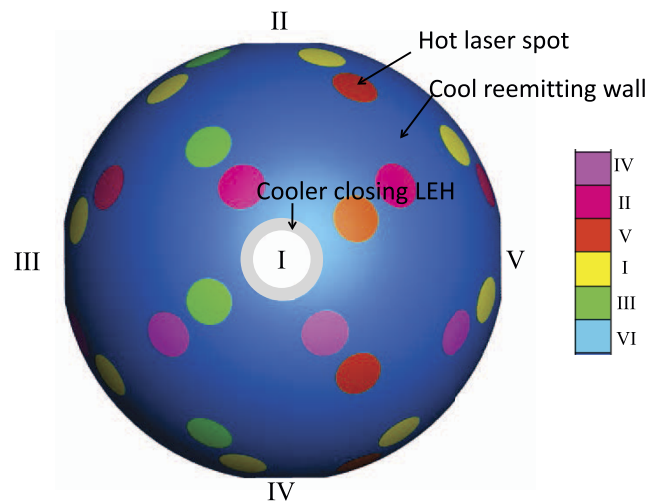


FIG. 2. Elevation of octahedral spherical hohlraum with its characteristic regions of hot laser spots, cool re-emitting wall, and cooler closing LEHs (gray). The LEHs are numbered, and the laser spots are colored according to these numbers. In this model, there are 48 laser quads with $\theta_l = 55^\circ$ and $\phi_{l0} = 11.25^\circ$. The hohlraum radius is $R_H = 5.5$ mm, the LEH radius is $R_{LEH} = 1$ mm, and the radius of the focal laser waist at the LEH is $R_Q = 0.6$ mm. LEH VI and the other 24 laser spots are on the opposite side.

whole radiation field inside the hohlraum and calculate the temporal and spectral radiation drive at any point on the capsule surface directly. The laser spot movement can be taken into consideration in the extended view factor model. This method had been successfully applied in analyzing an implosion experiment in an octahedral hohlraum.³⁹

IV. COMPARISON OF ENERGY EFFICIENCY BETWEEN OCTAHEDRAL AND CYLINDRICAL HOHLRAUMS

A. Will the six LEHs of an octahedral hohlraum lead to more radiation loss than the two LEHs of a cylindrical hohlraum?

In the fusion community, questions have often been asked regarding the radiation energy loss from an octahedral hohlraum with its six LEHs and concerns have been raised that such a hohlraum may lose much more radiation energy than a cylindrical hohlraum with just two LEHs. Here, it is worth mentioning that the radiation loss from a hohlraum is not determined by its LEH number, but by its total LEH area. Thus, the size of each LEH is key here. For a laser beam to be injected smoothly into an LEH, it is necessary that the LEH radius R_L satisfy

$$R_L \geq R_Q + \Delta + \varepsilon, \quad (1)$$

where R_Q is the beam size at the LEH, Δ is the LEH closure under radiation ablation, and ε is the laser pointing error. From a simple estimate^{28,29} obtained by taking $R_Q \sim 0.6$ mm, $\Delta \sim 0.28$ mm at 300 eV, and $\varepsilon \sim 0.08$ mm, we have $R_L \sim 1$ mm for an ignition-scale octahedral hohlraum. This result has been confirmed by our 2D simulations.⁷⁵

We proposed to use the prepulse of an ignition pulse to determine the LEH size of an ignition-scale hohlraum via LEH closure behavior and carried out experiments in 2017 and 2020 at SGIII.⁷⁶ Convincing evidence from multiple diagnostics again showed that $R_L \approx 1$ mm for $R_Q = 0.6$ mm, $\varepsilon \sim 0.08$ mm, and the prepulse used in the experiment. Thus, the total area of the six LEHs with $R_L = 1$ mm is similar to that of the two LEHs of the cylindrical hohlraums used in the NIF experiments,⁷⁷⁻⁷⁹ which indicates that octahedral hohlraums have similar radiation energy losses to cylindrical hohlraums. It might be asked why the NIF cylindrical hohlraums need much bigger LEHs. One of the reasons is that these hohlraums need much fatter inner beams^{80,81} to suppress their serious LPI. In addition, the LEH size of the NIF cylindrical hohlraums is usually taken as 50%–60% of the hohlraum radius owing to symmetry considerations.⁸²

B. Will a large hohlraum-to-capsule radius ratio of an octahedral hohlraum lead to a lower coupling efficiency than a cylindrical hohlraum?

In indirect drive, the energy coupling efficiency from the laser to an imploded central hot spot is the product of the laser absorption efficiency η_{al} of the hohlraum (mainly determined by LPI), the conversion efficiency η_{LX} from absorbed laser to x-rays (mainly determined by the wall materials), the coupling efficiency η_{HC} from hohlraum to capsule (mainly determined by the geometrical ratios

of hohlraum and capsule), and the energy coupling efficiency η_{CH} from capsule surface to hot spot (which varies with the capsule design and is sensitive to radiation asymmetry and target fabrication). Therefore, the energy finally transferred to the hot spot, E_{HS} , can be expressed as

$$E_{HS} = \eta_{al}\eta_{LX}\eta_{HC}\eta_{CH}E_L, \quad (2)$$

where E_L is the input laser energy.

Queries are often raised regarding η_{HC} of the octahedral hohlraum because the hohlraum-to-capsule radius ratio is usually taken as 3.7–5, obviously larger than the range of 2.55–4.2 for the cylindrical hohlraums of the NIF.^{6,20,80} First, it is worthy mentioning that it is the ratio of hohlraum area to capsule area that is directly related to η_{HC} , not the ratio of hohlraum radius to capsule radius. In addition, the cylindrical hohlraum is elongated, and so a length-to-diameter ratio should also be taken into consideration. We can express η_{HC} as:^{30,56}

$$\eta_{HC} = \frac{(1 - \alpha_C)A_C}{(1 - \alpha_W)A_W + (1 - \alpha_C)A_C + A_L}, \quad (3)$$

where α_C is the capsule albedo, α_W is the wall albedo, A_C is the capsule area, A_W is the hohlraum wall area, and A_L is the total area of all LEHs. We define $A_H = A_W + A_L$. From the above expression, it can be seen that η_{HC} is completely determined by A_H/A_C at given A_L and A_C . Keeping both A_L and A_C fixed, we present the variations of A_H/A_C vs R_H/R_C for the octahedral and cylindrical hohlraums in Fig. 3. As can be seen, octahedral hohlraums with $R_H/R_C = 3.8, 5,$ and 6.3 have the same A_H/A_C as cylindrical hohlraums with $R_H/R_C = 2.66, 3.33,$ and $4.2,$ respectively. Therefore, η_{HC} of the two kinds of hohlraums is similar within the respective reasonable ranges of R_H/R_C . In this paper, we take $\alpha_W = 0.86$ and $\alpha_C = 0.3$ as in Refs. 30 and 50. We calculate η_{HC} of the two kinds of

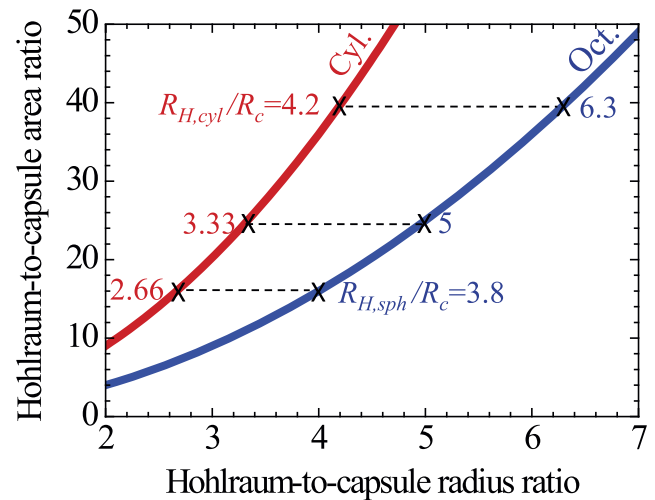


FIG. 3. A_H/A_C vs R_H/R_C for a cylindrical hohlraum (red line) and an octahedral hohlraum (blue line). Here, $R_{H,cyl}/R_C$ (red numbers) and $R_{H,oct}/R_C$ (blue numbers) are the hohlraum-to-capsule radius ratios of the cylindrical and octahedral hohlraums, respectively. The length-to-diameter ratio of the cylindrical hohlraum is taken as 1.75.

hohlraums for the capsule with $R_C = 1.195$ mm described in Ref. 19. From Eq. (2), we have $\eta_{HC} = 17.7\%$ for the cylindrical hohlraum with $L = 11.2$ mm, $R_{H,cyl} = 3.2$ mm, and $R_{L,cyl} = 1.82$ mm used in Ref. 19, and we have $\eta_{HC} = 18.2\%$ for an octahedral hohlraum with $R_{H,oct} = 4R_C$ and $R_{L,cyl} = 1$ mm. Again, η_{HC} is similar for the two kinds of hohlraums.

We can further examine the radiation asymmetry inside such an octahedral hohlraum. The radiation flux on the capsule surface can be expanded as $\sum_{l=0}^{\infty} \sum_{m=-l}^l a_{lm} Y_{lm}(\theta, \phi)$, where $Y_{lm}(\theta, \phi)$ is the spherical harmonic of the polar mode l (viewed from the equator) and the azimuthal mode m (viewed from the pole) and a_{lm} is the spherical harmonic decomposition. We define $C_{l0} = a_{l0}/a_{00}$ and $C_{lm} = 2a_{lm}/a_{00}$ for $m > 0$, and calculate C_{lm} with the 3D view factor code VF3D by taking the relative fluxes of the laser spot, hohlraum wall, and LEH as 2:1:0. Inside the above octahedral hohlraum with $R_{H,oct}/R_C = 4$ and $R_{L,oct}/R_C = 0.84$, VF3D gives $C_{2m} = 0$, $C_{lm} = 0$ for all odd l , $C_{40} = 0.36\%$, $C_{44} = 0.43\%$, $C_{80} = 4.8 \times 10^{-4}$, $C_{84} = 3.6 \times 10^{-4}$, and $C_{88} = 5.7 \times 10^{-4}$, without any symmetry tuning technology.

C. How about the laser absorption efficiency?

As mentioned above, the laser absorption efficiency is determined mainly by LPI. For the NIF cylindrical hohlraums, LPI of the inner beams is serious and considered to a major obstacle to achieving ignition,^{22,59} although LPI of the outer beams is low and acceptable. On average, according to Ref. 18, $\eta_{aL} \sim 84\% \pm 3\%$ over a wide range of laser parameters in the NIF cylindrical hohlraums filled with He gas with a density of 0.96 mg/cm³. In contrast to the complicated environment of a cylindrical hohlraum, an octahedral hohlraum with the ideal laser arrangement has a relatively simple and clean environment, with no beam crossing, no laser spot overlapping, and no interplay between laser beam propagation and ablated material from the capsule. In addition, the octahedral hohlraum also has the following advantages. First, the lasers enter the hohlraum at $\theta_L = 55^\circ$, with a shorter distance of laser propagation inside the hohlraum than lasers at a small θ_L , which is similar to the outer beams of the NIF cylindrical hohlraums. Second, the plasma filling inside a sphere is the lowest among all kinds of hohlraum configurations of the same area, because of the greatest volume of the sphere compared with all other configurations. Third, cylindrical LEHs can be used with an octahedral hohlraum to alleviate the potential influence of wall plasmas on laser transportation. All these advantages imply a lower LPI and hence a higher η_{aL} in octahedral hohlraums than in cylindrical hohlraums.

To experimentally compare LPI between spherical and cylindrical hohlraums, we performed experiments on the SGIII laser facility in 2015.^{37,38} The experimental results with the SGIII cylindrical hohlraums are similar to those from the NIF and indicated much higher LPI of the inner beams than the outer beams inside a gas-filled hohlraum. In particular, the experiments successfully demonstrated a low level of LPI in a spherical hohlraum for beams at $\theta_L = 55^\circ$, even with a capsule inside and filled with C₅H₁₂ gas at 0.9 mg/cm³. In 2017, we performed further LPI experiments in a spherical hohlraum at a high laser intensity at the ignition level. From our observations, we found that stimulated Raman scattering decreases with increasing laser intensity, while stimulated Brillouin scattering increases,

and the LPI fraction at 55° in a spherical hohlraum is lower than 8% at up to 1.73×10^{15} W/cm². Usually, we take $\eta_{aL} = 90\%$ for an octahedral hohlraum in estimating its required laser energy and power.

D. How about the energy efficiency from laser to hot spot?

The energy efficiency from laser to hot spot is given by the product $\eta_{aL}\eta_{LX}\eta_{HC}\eta_{CH}$. Among all these four efficiencies, η_{aL} , η_{LX} , and η_{HC} are relatively stable, while η_{CH} seems the most “elusive” and changeable, being quite sensitive to the symmetry of the radiation drive and to target fabrication. From the above discussions,

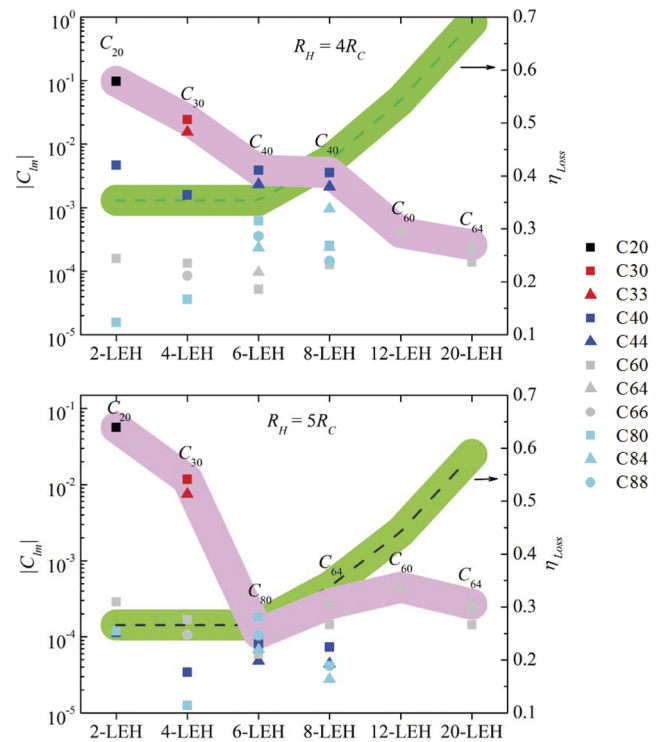


FIG. 4. Variations of C_{lm} (symbol) and η_{Loss} (dashed line, connected with the light green curve) with number of LEHs for spherical hohlraum of radius $R_H = 4R_C$ (upper) and $R_H = 5R_C$ (lower). Here, η_{Loss} is the energy loss efficiency via LEHs, defined as $\eta_{Loss} = A_L / [(1 - \alpha_W)A_W + (1 - \alpha_C)A_C + A_L]$. We take $R_L/R_C = 1.732$ for the 2-LEH spherical hohlraum, $R_L/R_C = 1.22$ for the 4-LEH hohlraum, and $R_L/R_C = 1$ for the 6-, 8-, 12-, and 20-LEH hohlraums. Thus, we take the same A_L for the spherical hohlraums with six and fewer LEHs, but the same R_L for the spherical hohlraums with six and more LEHs. Note that we take larger LEHs for the spherical hohlraums with two and four LEHs, because they both need lasers at multiple incident angles for symmetry tuning. A 4-LEH spherical hohlraum is usually called a tetrahedral hohlraum.^{29,56,85,86} With the same A_L , η_{Loss} is the same for the 2-, 4-, and 6-LEH hohlraums. For the hohlraums with more than six LEHs, η_{Loss} increases with increasing number of LEHs. The dominant C_{lm} 's of the spherical hohlraums with different numbers of LEHs are indicated on the figure and connected by the magenta curve. C_{2m} appears only for the 2-LEH hohlraum, and C_{3m} appears only for the 4-LEH hohlraum. For $R_H = 4R_C$, both 6- and 8-LEH spherical hohlraums are dominated by $C_{40} \sim 3.5 \times 10^{-3}$, but the 8-LEH has a remarkable higher η_{Loss} . For $R_H = 5R_C$, the 6-LEH spherical hohlraum is at its golden hohlraum-to-capsule radius ratio, dominated by $C_{80} \sim 1.1 \times 10^{-4}$, and its asymmetry is the lowest among all these hohlraums.

the cylindrical and octahedral hohlraums have the same or similar η_{LX} (~87%) and η_{HC} (10%–20%), while the octahedral hohlraum has a slight advantage in terms of η_{al} because of its lower LPI. We can roughly take $\eta_{al} \sim 85\%$ for the cylindrical hohlraum and $\sim 90\%$ for an octahedral hohlraum in an initial design.^{83,84} However, the octahedral hohlraum has an absolute advantage in terms of η_{CH} owing to its very high symmetry. It is η_{CH} that strongly influences the neutron yield in experiments, or the ratio of the measured neutron yield to the 1D-calculated neutron yield, often called the “yield over clean” (YOC). Between a good and a bad symmetry, η_{CH} and YOC can jump by orders of magnitude. In other words, it is the high symmetry of the octahedral hohlraum that makes η_{CH} much more stable, and hence increases the predictability and reproducibility of fusion gain, with the uncertainties being left to engineering.

In fact, as shown in Fig. 4, among all spherical hohlraums with different number of LEHs, the octahedral hohlraum gives the best tradeoff between radiation symmetry and energy coupling efficiency. From the point designs,^{75,87,88} the required laser energy for an octahedral hohlraum is within the capabilities of currently available laser facilities.

V. DESIGN ISLAND OF OCTAHEDRAL HOHLRAUM

As mentioned above, the radiation asymmetry of an octahedral hohlraum is determined mainly by R_H/R_C and R_L/R_C . In fact, from Eq. (3), η_{HC} of an octahedral hohlraum is also determined by these two ratios at given albedos. Together with the requirement on R_L from Eq. (1), we can define a design island of octahedral hohlraum in the plane of R_H/R_C and R_L/R_C by considering the limitations on C_{lm} and η_{HC} of an ignition target. We assume the following limitations: (1) $C_{40} \leq 0.8\%$ at the initial time $t = 0$; (2) $C_{40} \leq 0.8\%$ at the time at which $R_{C^*}/R_C = 0.25$; (3) $\eta_{HC} \geq 10\%$; and (4) $R_L/R_C \geq 0.8$. We then obtain the design island shown in Fig. 5. Here, we denote by R_{C^*} the radius of an imploding capsule of initial radius R_C . We consider the limitation on asymmetry given by $R_{C^*}/R_C = 0.25$, because a capsule is usually compressed 3–4 times in radius at the end of an ignition laser pulse according to our simulations, and, furthermore, the smoothing factor^{2,3,56} of C_{4m} changes little at $R_H/R_C > 10$. With a stringent limitation on asymmetry at both the initial time and the end of the laser pulse, it is possible to maintain high symmetry during the whole implosion process. The limitation on R_L is related to the details of ignition target design and laser facility, including the laser beam sizes, LPs, LEH closure, and laser beam pointing error. Here, we take $R_L/R_C \geq 0.8$ just as an example. We consider the limitation to C_{40} , whose absolute value is larger than $C_{4\pm 4}$. Here, it is worth mentioning that the mode $Y_{4\pm 4}$ has completely different polar and azimuthal angle ranges from the mode Y_{40} , and so C_{40} and $C_{4\pm 4}$ should not be added together. Finally, inside the design island, there is a region (blue in Fig. 5) where $C_{40} \leq 0.1\%$, and inside this region, $C_{4m} = 0$ at the golden radius ratio of $R_H/R_C \sim 5$.

As an example, we consider an octahedral hohlraum for the CH Rev5 ignition capsule of the NIF and estimate its asymmetry and required laser energy E_L . From Ref. 80, the CH Rev5 capsule has $R_C = 1.108$ mm and $E_C = 165$ kJ. For an octahedral hohlraum with $R_H/R_C = 4$ and $R_L/R_C = 1$, we have $C_{40} \sim 4 \times 10^{-3}$ at $t = 0$ and

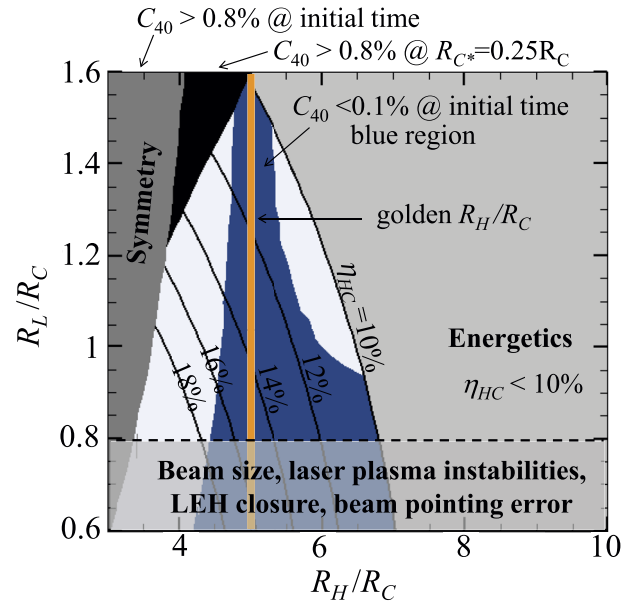


FIG. 5. Design island (surrounded by gray and black regions) of an octahedral spherical hohlraum in the plane of R_H/R_C and R_L/R_C . In the blue region, $C_{40} \leq 0.1\%$. The golden line corresponds to the golden radius ratio $R_H/R_C \sim 5$ with $C_{4m} = 0$. Outside the design island, $C_{40} > 0.8\%$ at $t = 0$ (dark gray region), $C_{40} > 0.8\%$ at $R_{C^*}/R_C = 0.25$ (black region), $\eta_{HC} < 10\%$ (light gray region), and $R_L/R_C < 0.8$ (transparent gray region).

$C_{40} \sim 5 \times 10^{-3}$ at $R_{C^*}/R_C = 0.25$ from VF3D, and $\eta_{HC} \sim 18\%$ from Eq. (3). We then have $E_L = E_C/\eta_{al}\eta_{LX}\eta_{HC} \sim 1.2$ MJ by taking $\eta_{al} = 90\%$ and $\eta_{LX} = 87\%$. For the case of $R_H/R_C = 5$ and $R_L/R_C = 0.9$, we have $C_{40} \sim 9 \times 10^{-5}$ at $t = 0$, $C_{40} \sim 3 \times 10^{-3}$ at $R_{C^*}/R_C = 0.25$, $\eta_{HC} \sim 13.3\%$, and $E_L \sim 1.6$ MJ. Note that η_{HC} varies with α_W and α_C , while α_W and α_C are functions of the target material and radiation pulse. The albedos should be adjusted to match experiments to estimate E_L more accurately.

VI. CHALLENGES AND TASKS

From a physics-based viewpoint, an octahedral hohlraum can realize an ideal and clear drive without the use of symmetry tuning technology, with the remaining uncertainties of fusion gain moved to engineering. To achieve dream fusion, there are still many challenges in the path forward. The following tasks are worthy of efforts.

1. A fusion laser facility should be constructed with the ideal laser arrangement for an octahedral hohlraum.
2. A target chamber with octahedral configuration should be designed and constructed, the diagnostics for which should address the important physical quantities of all kinds of characteristic region inside the octahedral hohlraum. Here, the capsule is also regarded as a characteristic region.
3. Key diagnostics should be developed, with high spatial, temporal, and spectral resolutions.⁸⁹ These need to be such that

their fields of view cover several LEHs⁹⁰ or such that they can be focused on the small size of a characteristic region.⁹¹

- Novel capsule support methods that can retain the perfect symmetry of the octahedral hohlraum should be explored, for example, the use of superconducting magnetic levitation.⁹²
- The fabrication of beryllium or beryllium-based capsules needs to be improved to provide superior ablation properties^{93–95} that can be fully exploited inside the ideal radiation environment of an octahedral hohlraum.⁸⁷
- Optimum target designs with unconventional ablator capsules, such as aluminum capsules⁹⁶ or the recently proposed HDC-CH capsules,⁸⁸ with nonequilibrium between ions and electrons in the hot spot,⁹⁷ should be investigated.
- Hohlraum walls with special structures, such as sandwich walls,^{98,99} foam walls,^{100–102} or honeycomb walls, should be investigated with the aim of increasing the laser absorption efficiency. Honeycomb walls differ from foam walls in their density requirement. There is no requirement on the density of a honeycomb wall, whereas foam walls must usually have a density less than 0.5 g/cm³.
- An extended view factor model should be developed, with input consisting of the measured radiation from all characteristic regions and output consisting of the 3D spatial, temporal, and spectral characteristics of the radiation drive.
- A 3D Monte Carlo radiation hydrodynamic code³¹ with more accurate physics models^{103–110} should be developed for the octahedral hohlraum to improve target design and reveal details of novel physics.
- Novel laser technologies with high laser absorption efficiency and low LPI, including but not limited to broadband^{111,112} or sunlight-like lasers,¹¹³ should be developed for lasers at those wavelengths with a high damage threshold for optical components, such as lasers at 0.53 μm ^{101,102} or even longer wavelengths, to greatly increase the daily shot number operation at the full energy of a laser facility.
- Finally, besides indirect drive, target designs for direct-drive, hybrid-drive, and laser-driven spherically convergent plasma fusion should be explored on the octahedral-configured fusion laser facility.

In summary, the octahedral hohlraum provides an ideal and practice approach for the next generation of laser systems to achieve predictable and reproducible fusion gain via multiple schemes. This may open a new era in the development of controlled nuclear fusion and aid progress toward the realization of an airbus era of controlled nuclear fusion and laser inertial fusion energy power plants.

ACKNOWLEDGMENTS

The author appreciate the entire octahedral spherical hohlraum team at the Institute of Applied Physics and Computational Mathematics in Beijing and the Research Center of Laser Fusion in Mianyang for their outstanding work in theory, simulation, experiment, diagnostics, and laser operations in studies of octahedral spherical hohlraums. The author also thanks Dr. Hui Cao for his help with Figs. 2 and 4. This work is supported by the National Natural Science Foundation of China (Grant No. 12035002).

AUTHOR DECLARATIONS

Conflict of Interest

The author has no conflicts to disclose.

Author Contributions

Ke Lan: Conceptualization (equal); Writing – original draft (equal); Writing – review & editing (equal).

DATA AVAILABILITY

The data that support the findings of this study are available from the corresponding author upon reasonable request.

REFERENCES

- J. Nuckolls, L. Wood, A. Thiessen, and G. Zimmerman, "Laser compression of matter to super-high densities: Thermonuclear (CTR) applications," *Nature* **239**, 139 (1972).
- J. Lindl, "Development of the indirect-drive approach to inertial confinement fusion and the target physics basis for ignition and gain," *Phys. Plasmas* **2**, 3933 (1995).
- S. Atzeni and J. Meyer-ter-Vehn, *The Physics of Inertial Fusion* (Oxford Science, Oxford, 2004).
- E. M. Campbell and W. J. Hogan, "The National Ignition Facility—Applications for inertial fusion energy and high-energy-density science," *Plasma Phys. Controlled Fusion* **41**, B39 (1999).
- J. D. Lindl and E. I. Moses, "Special Topic: Plans for the National Ignition Campaign (NIC) on the National Ignition Facility (NIF): On the threshold of initiating ignition experiments," *Phys. Plasmas* **18**, 050901 (2011).
- S. Le Pape, L. F. Berzak Hopkins, L. Divol, A. Pak, E. L. Dewald, S. Bhandarkar, L. R. Benedetti, T. Bunn, J. Biener, J. Crippen *et al.*, "Fusion energy output greater than the kinetic energy of an imploding shell at the National Ignition Facility," *Phys. Rev. Lett.* **120**, 245003 (2018).
- D. Clery, "Laser-powered fusion effort nears, 'ignition,'" *Science* **373**, 841 (2021).
- H. Abu-Shawareb, R. Acree, P. Adams, J. Adams, B. Addis, R. Aden *et al.*, "Lawson criterion for ignition exceeded in an inertial fusion experiment," *Phys. Rev. Lett.* **129**, 075001 (2022).
- A. B. Zylstra, A. L. Kritcher, O. A. Hurricane, D. A. Callahan, J. E. Ralph, D. T. Casey *et al.*, "Experimental achievement and signatures of ignition at the National Ignition Facility," *Phys. Rev. E* **106**, 025202 (2022).
- A. L. Kritcher, A. B. Zylstra, D. A. Callahan, O. A. Hurricane, C. R. Weber, D. S. Clark *et al.*, "Design of an inertial fusion experiment exceeding the Lawson criterion for ignition," *Phys. Rev. E* **106**, 025201 (2022).
- P. Michel, L. Divol, E. A. Williams, S. Weber, C. A. Thomas, D. A. Callahan *et al.*, "Tuning the implosion symmetry of ICF targets via controlled crossed-beam energy transfer," *Phys. Rev. Lett.* **102**, 025004 (2009).
- R. P. J. Town, D. K. Bradley, A. Kritcher, O. S. Jones, J. R. Rygg, R. Tommasini *et al.*, "Dynamic symmetry of indirectly driven inertial confinement fusion capsules on the National Ignition Facility," *Phys. Plasmas* **21**, 056313 (2014).
- A. L. Kritcher, R. Town, D. Bradley, D. Clark, B. Spears, O. Jones *et al.*, "Metrics for long wavelength asymmetries in inertial confinement fusion implosions on the National Ignition Facility," *Phys. Plasmas* **21**, 042708 (2014).
- L. Divol, A. Pak, L. F. Berzak Hopkins, S. L. Pape, N. B. Meezan, E. L. Dewald *et al.*, "Symmetry control of an indirectly driven high-density-carbon implosion at high convergence and high velocity," *Phys. Plasmas* **24**, 056309 (2017).
- D. A. Callahan, O. A. Hurricane, J. E. Ralph, C. A. Thomas, K. L. Baker, L. R. Benedetti *et al.*, "Exploring the limits of case-to-capsule ratio, pulse length, and picket energy for symmetric hohlraum drive on the National Ignition Facility laser," *Phys. Plasmas* **25**, 056305 (2018).

- ¹⁶A. L. Kritcher, D. E. Hinkel, D. A. Callahan, O. A. Hurricane, D. Clark, D. T. Casey *et al.*, “Integrated modeling of cryogenic layered highfoot experiments at the NIF,” *Phys. Plasmas* **23**, 052709 (2016).
- ¹⁷O. S. Jones, C. J. Cerjan, M. M. Marinak, J. L. Milovich, H. F. Robey, P. T. Springer *et al.*, “A high-resolution integrated model of the National Ignition Campaign cryogenic layered experiments,” *Phys. Plasmas* **19**, 056315 (2012).
- ¹⁸J. L. Kline, D. A. Callahan, S. H. Glenzer, N. B. Meezan, J. D. Moody, D. E. Hinkel *et al.*, “Hohlraum energetics scaling to 520 TW on the National Ignition Facility,” *Phys. Plasmas* **20**, 056314 (2013).
- ¹⁹A. B. Zylstra, O. A. Hurricane, D. A. Callahan, A. L. Kritcher, J. E. Ralph, H. F. Robey *et al.*, “Burning plasma achieved in inertial fusion,” *Nature* **601**, 542 (2022).
- ²⁰S. A. MacLaren, L. P. Masse, C. E. Czajka, S. F. Khan, G. A. Kyrala, T. Ma *et al.*, “A near one-dimensional indirectly driven implosion at convergence ratio 30,” *Phys. Plasmas* **25**, 056311 (2018).
- ²¹G. Ren, J. Liu, W. Huo, and K. Lan, “Analysis of hohlraum energetics of the SG series and the NIF experiments with energy balance model,” *Matter Radiat. Extremes* **2**, 22 (2017).
- ²²J. Lindl, O. Landen, J. Edwards, E. Moses, and NIC Team, “Review of the National Ignition Campaign 2009-2012,” *Phys. Plasmas* **21**, 020501 (2014).
- ²³National Nuclear Security Administration, “2015 review of the inertial confinement fusion and high energy density science portfolio: Volume I,” Report No. DOE/NA-0040, May, 2016.
- ²⁴Lawrence Livermore National Laboratory, “Lasers indirect drive input to NNSA 2020 report,” Report No. LLNL-TR-810573, May, 2020.
- ²⁵J.-L. Miquel and E. Prene, “LMJ & PETAL status and program overview,” *Nucl. Fusion* **59**, 032005 (2019).
- ²⁶W. Zheng, X. Wei, Q. Zhu, F. Jing, D. Hu, X. Yuan *et al.*, “Laser performance upgrade for precise ICF experiment in SG-III laser facility,” *Matter Radiat. Extremes* **2**, 243 (2017).
- ²⁷K. Lan, J. Liu, D. Lai, W. Zheng, and X.-T. He, “High flux symmetry of the spherical hohlraum with octahedral 6LEHs at a golden hohlraum-to-capsule radius ratio,” arXiv:1311.1263v2 (2013).
- ²⁸K. Lan, J. Liu, D. Lai, W. Zheng, and X.-T. He, “High flux symmetry of the spherical hohlraum with octahedral 6LEHs at a golden hohlraum-to-capsule radius ratio,” *Phys. Plasmas* **21**, 010704 (2014).
- ²⁹K. Lan, X.-T. He, J. Liu, W. Zheng, and D. Lai, “Octahedral spherical hohlraum and its laser arrangement for inertial fusion,” *Phys. Plasmas* **21**, 052704 (2014).
- ³⁰K. Lan and W. Zheng, “Novel spherical hohlraum with cylindrical laser entrance holes and shields,” *Phys. Plasmas* **21**, 090704 (2014).
- ³¹S. Li, K. Lan, and J. Liu, “Study on size of laser entrance hole shield for ignition octahedral spherical hohlraums,” *Laser Part. Beams* **33**, 731 (2015).
- ³²W. Huo, Z. Li, D. Yang, K. Lan, J. Liu, G. Ren *et al.*, “First demonstration of improving laser propagation inside the spherical hohlraums by using the cylindrical laser entrance hole,” *Matter Radiat. Extremes* **1**, 2 (2016).
- ³³Z. Li, D. Yang, S. Li, W. Y. Huo, K. Lan, J. Liu, G. Ren *et al.*, “Comparison of the laser spot movement inside cylindrical and spherical hohlraums,” *Phys. Plasmas* **24**, 072711 (2017).
- ³⁴W. Y. Huo, Z. Li, Y. H. Chen, X. Xie, K. Lan, J. Liu *et al.*, “First investigation on the radiation field of the spherical hohlraum,” *Phys. Rev. Lett.* **117**, 025002 (2016).
- ³⁵X. Xie, Z. Li, S. Li, Y. Huang, L. Jing, D. Yang *et al.*, “Radiation flux study of spherical hohlraums at the SGIII prototype facility,” *Phys. Plasmas* **23**, 112701 (2016).
- ³⁶W. Y. Huo, Z. Li, Y.-H. Chen, X. Xie, G. Ren, H. Cao *et al.*, “First octahedral spherical hohlraum energetics experiment at the SGIII laser facility,” *Phys. Rev. Lett.* **120**, 165001 (2018).
- ³⁷K. Lan, Z. Li, X. Xie, Y. H. Chen, C. Zheng, C. Zhai *et al.*, “Experimental demonstration of low laser-plasma instabilities in gas-filled spherical hohlraums at laser injection angle designed for ignition target,” *Phys. Rev. E* **95**, 031202 (2017).
- ³⁸Y. Chen, Z. Li, X. Xie, C. Zheng, C. Zhai, L. Hao *et al.*, “First experimental comparisons of laser-plasma interactions between spherical and cylindrical hohlraums at SGIII laser facility,” *Matter Radiat. Extremes* **2**, 77 (2017).
- ³⁹K. Lan, Y. Dong, J. Wu, Z. Li, Y. Chen, H. Cao *et al.*, “First inertial confinement fusion implosion experiment in octahedral spherical hohlraum,” *Phys. Rev. Lett.* **127**, 245001 (2021).
- ⁴⁰S. Jiang, L. Jing, Y. Huang, and Y. Ding, “Novel free-form hohlraum shape design and optimization for laser-driven inertial confinement fusion,” *Phys. Plasmas* **21**, 102710 (2014).
- ⁴¹H. Duan, C. Wu, W. Pei, and S. Zou, “Theoretical study of symmetry of flux onto a capsule,” *Phys. Plasmas* **22**, 092704 (2015).
- ⁴²L. Ren, D. Zhao, and J. Zhu, “Beam guiding system geometric arrangement in the target area of high-power laser drivers,” *High Power Laser Sci. Eng.* **3**, e12 (2015).
- ⁴³S. Jiang, Y. Huang, L. Jing, H. Li, T. Huang, and Y. Ding, “A unified free-form representation applied to the shape optimization of the hohlraum with octahedral 6 laser entrance holes,” *Phys. Plasmas* **23**, 012702 (2016).
- ⁴⁴H. Duan, C. Wu, W. Pei, and S. Zou, “Instability analysis of pointing accuracy and power imbalance of spherical hohlraum,” *Phys. Plasmas* **23**, 052703 (2016).
- ⁴⁵S. Jiang, L. Jing, Y. Huang, H. Li, T. Huang, and Y. Ding, “A spherical hohlraum design with tetrahedral 4 laser entrance holes and high radiation performance,” *Phys. Plasmas* **23**, 122703 (2016).
- ⁴⁶L. Kuang, H. Li, L. Jing, Z. Lin, L. Zhang, L. Li, Y. Ding, S. Jiang, J. Liu, and J. Zheng, “A novel three-axis cylindrical hohlraum designed for inertial confinement fusion ignition,” *Sci. Rep.* **6**, 34636 (2016).
- ⁴⁷X. Li, C.-S. Wu, Z.-S. Dai, W.-D. Zheng, J.-F. Gu, P.-J. Gu, S.-Y. Zou, J. Liu, and S.-P. Zhu, “A new ignition hohlraum design for indirect-drive inertial confinement fusion,” *Chin. Phys. B* **25**, 085202 (2016).
- ⁴⁸L. Jing, S. Jiang, L. Kuang, L. Zhang, L. Li, Z. Lin *et al.*, “Preliminary study on a tetrahedral hohlraum with four half-cylindrical cavities for indirectly driven inertial confinement fusion,” *Nucl. Fusion* **57**, 046020 (2017).
- ⁴⁹P. E. Masson-Laborde, M. C. Monteil, V. Tassin, F. Philippe, P. Gauthier, A. Casner *et al.*, “Laser plasma interaction on rugby hohlraum on the Omega Laser Facility: Comparisons between cylinder, rugby, and elliptical hohlraums,” *Phys. Plasmas* **23**, 022703 (2016).
- ⁵⁰W. A. Farmer, M. Tabak, J. H. Hammer, P. A. Amendt, and D. E. Hinkel, “High-temperature hohlraum designs with multiple laser-entrance holes,” *Phys. Plasmas* **26**, 032701 (2019).
- ⁵¹W. Wang and R. S. Craxton, “Development of a beam configuration for the SG4 laser to support both direct and indirect drive,” August 2020, https://www.ile.rochester.edu/media/publications/high_school_reports/documents/hs_reports/2019/Wang_William.pdf.
- ⁵²S. Craxton, “A new beam configuration to support both spherical hohlraums and symmetric direct drive,” in The 62nd Annual Meeting of the American Physical Society Division of Plasma Physics, 9–13 November 2020.
- ⁵³W. Y. Wang and R. S. Craxton, “Pentagonal prism spherical hohlraums for OMEGA,” *Phys. Plasmas* **28**, 062703 (2021).
- ⁵⁴W. Y. Wang and R. S. Craxton, “A proposal for pentagonal prism spherical hohlraum experiments on OMEGA,” *LLE Review*, **166**, Jan-Mar 2021.
- ⁵⁵X. Li, Y. Dong, D. Kang, W. Jiang, H. Shen, L. Kuang *et al.*, “First indirect drive experiment using a six-cylinder-port hohlraum,” *Phys. Rev. Lett.* **128**, 195001 (2022).
- ⁵⁶K. Lan, J. Liu, Z. Li, X. Xie, W. Huo, Y. Chen *et al.*, “Progress in octahedral spherical hohlraum study,” *Matter Radiat. Extremes* **1**, 8 (2016).
- ⁵⁷J. D. Lindl, P. Amendt, R. L. Berger, S. G. Glendinning, S. H. Glenzer, S. W. Haan, R. L. Kauffman, O. L. Landen, and L. J. Suter, “The physics basis for ignition using indirect-drive targets on the National Ignition Facility,” *Phys. Plasmas* **11**, 339 (2004).
- ⁵⁸W. Y. Huo, J. Liu, Y. Zhao, W. Zheng, and K. Lan, “Insensitivity of the octahedral spherical hohlraum to power imbalance, pointing accuracy, and assemblage accuracy,” *Phys. Plasmas* **21**, 114503 (2014).
- ⁵⁹J. D. Moody, D. A. Callahan, D. E. Hinkel, P. A. Amendt, K. L. Baker, D. Bradley *et al.*, “Progress in hohlraum physics for the National Ignition Facility,” *Phys. Plasmas* **21**, 056317 (2014).
- ⁶⁰J. F. Myatt, J. Zhang, R. W. Short, A. V. Maximov, W. Seka, D. H. Froula *et al.*, “Multiple-beam laser-plasma interactions in inertial confinement fusion,” *Phys. Plasmas* **21**, 055501 (2014).

- ⁶¹D. J. Strozzi, D. S. Bailey, P. Michel, L. Divol, S. M. Sepke, G. D. Kerbel, C. A. Thomas, J. E. Ralph, J. D. Moody, and M. B. Schneider, "Interplay of laser-plasma interactions and inertial fusion hydrodynamics," *Phys. Rev. Lett.* **118**, 025002 (2017).
- ⁶²E. M. Campbell, V. N. Goncharov, T. C. Sangster, S. P. Regan, P. B. Radha, R. Betti *et al.*, "Laser-direct-drive program: Promise, challenge, and path forward," *Matter Radiat. Extremes* **2**, 37 (2017).
- ⁶³X. T. He, J. W. Li, Z. F. Fan, L. F. Wang, J. Liu, K. Lan, J. F. Wu, and W. H. Ye, "A hybrid-drive nonisobaric-ignition scheme for inertial confinement fusion," *Phys. Plasmas* **23**, 082706 (2016).
- ⁶⁴G. Ren, J. Yan, J. Liu, K. Lan, Y. H. Chen, W. Y. Huo *et al.*, "Neutron generation by laser-driven spherically convergent plasma fusion," *Phys. Rev. Lett.* **118**, 165001 (2017).
- ⁶⁵M. Liu, X. Ai, Y. Liu, Q. Chen, S. Zhang, Z. He, Y. Huang, and Q. Yin, "Fabrication of solid CH-CD multilayer microspheres for inertial confinement fusion," *Matter Radiat. Extremes* **6**, 025901 (2021).
- ⁶⁶M. H. Emery, J. H. Orens, J. H. Gardner, and J. P. Boris, "Influence of nonuniform laser intensities on ablatively accelerated targets," *Phys. Rev. Lett.* **48**, 253 (1982).
- ⁶⁷S. Skupsky and K. Lee, "Uniformity of energy deposition for laser driven fusion," *J. Appl. Phys.* **54**, 3662 (1983).
- ⁶⁸S. Kawata and K. Niu, "Effect of nonuniform implosion of target on fusion parameters," *J. Phys. Soc. Jpn.* **53**, 3416 (1984).
- ⁶⁹V. N. Goncharov, S. Skupsky, T. R. Boehly, J. P. Knauer, P. McKenty, V. A. Smalyuk, R. P. J. Town, O. V. Gotchev, R. Betti, and D. D. Meyerhofer, "A model of laser imprinting," *Phys. Plasmas* **7**, 2062 (2000).
- ⁷⁰R. L. Kauffman, L. J. Suter, C. B. Darrow, J. D. Kilkenny, H. N. Kornblum, D. S. Montgomery *et al.*, "High temperatures in inertial confinement fusion radiation cavities heated with 0.35 μm light," *Phys. Rev. Lett.* **73**, 2320 (1994).
- ⁷¹D. S. Clark, C. R. Weber, J. L. Milovich, A. E. Pak, D. T. Casey, B. A. Hammel *et al.*, "Three-dimensional modeling and hydrodynamic scaling of National Ignition Facility implosions," *Phys. Plasmas* **26**, 050601 (2019).
- ⁷²S. A. MacLaren, M. B. Schneider, K. Widmann, J. H. Hammer, B. E. Yoxall, J. D. Moody *et al.*, "Novel characterization of capsule X-ray drive at the National Ignition Facility," *Phys. Rev. Lett.* **112**, 105003 (2014).
- ⁷³W. Y. Huo, K. Lan, Y. Li, D. Yang, S. Li, X. Li *et al.*, "Determination of the hohlraum M-band fraction by a shock-wave technique on the SGIII-prototype laser facility," *Phys. Rev. Lett.* **109**, 145004 (2012).
- ⁷⁴A. Caruso and C. Strangio, "The quality of the illumination for a spherical capsule enclosed in a radiating cavity," *Jpn. J. Appl. Phys.* **30**, 1095 (1991).
- ⁷⁵H. Cao, Y.-H. Chen, C. Zhai, C. Zheng, and K. Lan, "Design of octahedral spherical hohlraum for CH Rev5 ignition capsule," *Phys. Plasmas* **24**, 082701 (2017).
- ⁷⁶Y. Chen, Z. Li, H. Cao, K. Pan, S. Li, X. Xie *et al.*, "Demonstration of the feasibility of octahedral spherical hohlraum for inertial confinement fusion" (submitted).
- ⁷⁷L. F. Berzak Hopkins, N. B. Meezan, S. Le Pape, L. Divol, A. J. Mackinnon, D. D. Ho *et al.*, "First high-convergence cryogenic implosion in a near-vacuum hohlraum," *Phys. Rev. Lett.* **114**, 175001 (2015).
- ⁷⁸A. L. Kritcher, A. B. Zylstra, D. A. Callahan, O. A. Hurricane, C. Weber, J. Ralph *et al.*, "Achieving record hot spot energies with large HDC implosions on NIF in HYBRID-E," *Phys. Plasmas* **28**, 072706 (2021).
- ⁷⁹A. L. Kritcher, C. V. Young, H. F. Robey, C. R. Weber, A. B. Zylstra, O. A. Hurricane *et al.*, "Design of inertial fusion implosions reaching the burning plasma regime," *Nat. Phys.* **18**, 251–258 (2022).
- ⁸⁰S. W. Haan, J. D. Lindl, D. A. Callahan, D. S. Clark, J. D. Salmonson, B. A. Hammel *et al.*, "Point design targets, specifications, and requirements for the 2010 ignition campaign on the National Ignition Facility," *Phys. Plasmas* **18**, 051001 (2011).
- ⁸¹M. B. Schneider, S. A. MacLaren, K. Widmann, N. B. Meezan, J. H. Hammer, B. E. Yoxall *et al.*, "The size and structure of the entrance hole in gas-filled hohlraums at the National Ignition Facility," *Phys. Plasmas* **22**, 122705 (2015).
- ⁸²D. E. Hinkel, D. A. Callahan, A. B. Langdon, S. H. Langer, C. H. Still, and E. A. Williams, "Analyses of laser-plasma interactions in National Ignition Facility ignition targets," *Phys. Plasmas* **15**, 056314 (2008).
- ⁸³K. Lan, P. Gu, G. Ren, X. Li, C. Wu, W. Huo, D. Lai, and X.-T. He, "An initial design of hohlraum driven by a shaped laser pulse," *Laser Part. Beams* **28**, 421 (2010).
- ⁸⁴K. Lan, D. Lai, Y. Zhao, and X. Li, "Initial study and design on ignition ellipraum," *Laser Part. Beams* **30**, 175 (2012).
- ⁸⁵D. W. Phillion and S. M. Pollaine, "Dynamical compensation of irradiation nonuniformities in a spherical hohlraum illuminated with tetrahedral symmetry by laser beams," *Phys. Plasmas* **1**, 2963 (1994).
- ⁸⁶J. M. Wallace, T. J. Murphy, N. D. Delamater, K. A. Klare, J. A. Oertel, G. R. Magelssen, E. L. Lindman, A. A. Hauer, and P. Gobby, "Inertial confinement fusion with tetrahedral hohlraums at OMEGA," *Phys. Rev. Lett.* **82**, 3807 (1999).
- ⁸⁷G. Ren, K. Lan, Y.-H. Chen, Y. Li, C. Zhai, and J. Liu, "Octahedral spherical hohlraum for Rev. 6 NIF beryllium capsule," *Phys. Plasmas* **25**, 102701 (2018).
- ⁸⁸X. Qiao and K. Lan, "Novel target designs to mitigate hydrodynamic instabilities growth in inertial confinement fusion," *Phys. Rev. Lett.* **126**, 185001 (2021).
- ⁸⁹F. Wang, S. Jiang, Y. Ding, S. Liu, J. Yang, S. Li *et al.*, "Recent diagnostic developments at the 100 kJ-level laser facility in China," *Matter Radiat. Extremes* **5**, 035201 (2020).
- ⁹⁰Q. Wang *et al.*, "Development of a gated X-ray imager with multiple views and spectral selectivity for observing plasmas evolution in hohlraums," *Rev. Sci. Instrum.* **90**, 073301 (2019).
- ⁹¹K. Ren, S. Liu, L. Hou, H. Du, G. Ren, W. Huo *et al.*, "Direct measurement of x-ray flux for a pre-specified highly-resolved region in hohlraum," *Opt. Express* **23**, A1072 (2015).
- ⁹²X. Li, T. Xiao, F. Chen *et al.*, "A novel superconducting magnetic levitation method to support the laser fusion capsule by using permanent magnets," *Matter Radiat. Extremes* **3**, 104 (2018).
- ⁹³D. C. Wilson, P. A. Bradley, N. M. Hoffman, F. J. Swenson, D. P. Smitherman, R. E. Chrien *et al.*, "The development and advantages of beryllium capsules for the National Ignition Facility," *Phys. Plasmas* **5**, 1953 (1998).
- ⁹⁴R. E. Olson, G. A. Rochau, O. L. Landen, and R. J. Leeper, "X-ray ablation rates in inertial confinement fusion capsule materials," *Phys. Plasmas* **18**, 032706 (2011).
- ⁹⁵J. L. Kline, S. A. Yi, A. N. Simakov, R. E. Olson, D. C. Wilson, G. A. Kyrala, T. S. Perry, S. H. Batha, A. B. Zylstra, E. L. Dewald *et al.*, "First beryllium capsule implosions on the National Ignition Facility," *Phys. Plasmas* **23**, 056310 (2016).
- ⁹⁶J. L. Kline and J. D. Hager, "Aluminum X-ray mass-ablation rate measurements," *Matter Radiat. Extremes* **2**, 16 (2017).
- ⁹⁷Z. Fan, Y. Liu, B. Liu, C. Yu, K. Lan, and J. Liu, "Non-equilibrium between ions and electrons inside hot spots from National Ignition Facility experiments," *Matter Radiat. Extremes* **2**, 3 (2017).
- ⁹⁸X. Li, K. Lan, X. Meng, X. He, D. Lai, and T. Feng, "Study on Au + U + Au sandwich hohlraum wall for ignition targets," *Laser Part. Beams* **28**, 75 (2010).
- ⁹⁹L. Guo, Y. Ding, P. Xing, S. Li, L. Kuang, Z. Li, T. Yi, G. Ren, Z. Wu, L. Jing *et al.*, "Uranium hohlraum with an ultrathin uranium-nitride coating layer for low hard x-ray emission and high radiation temperature," *New J. Phys.* **17**, 113004 (2015).
- ¹⁰⁰M. D. Rosen and J. H. Hammer, "Analytic expressions for optimal inertial-confinement fusion hohlraum wall density and wall loss," *Phys. Rev. E* **72**, 056403 (2005).
- ¹⁰¹K. Lan and P. Song, "Foam Au driven by 4ω - 2ω ignition laser pulse for inertial confinement fusion," *Phys. Plasmas* **24**, 052707 (2017).
- ¹⁰²Y.-H. Chen, K. Lan, W. Zheng, and E. M. Campbell, "High coupling efficiency of foam spherical hohlraum driven by 2ω laser light," *Phys. Plasmas* **25**, 022702 (2018).
- ¹⁰³P. D. Nicolai, J.-L. A. Feugeas, and G. P. Schurtz, "A practical non-local model for heat transport in magnetized laser plasmas," *Phys. Plasmas* **13**, 032701 (2006).
- ¹⁰⁴W. Y. Huo, K. Lan, P. J. Gu, H. Yong, and Q. H. Zeng, "Electron heat conduction under non-Maxwellian distribution in hohlraum simulation," *Phys. Plasmas* **19**, 012313 (2012).

- ¹⁰⁵K. Lan, X. Qiao, P. Song, W. Zheng, B. Qing, and J. Zhang, “Study on laser-irradiated Au plasmas by detailed configuration accounting atomic physics,” *Phys. Plasmas* **24**, 102706 (2017).
- ¹⁰⁶J. Nikl, M. Holec, M. Zeman, M. Kuchařík, J. Limpouch, and S. Weber, “Macroscopic laser-plasma interaction under strong non-local transport conditions for coupled matter and radiation,” *Matter Radiat. Extremes* **3**, 110 (2018).
- ¹⁰⁷K. Li and K. Lan, “Escape of α -particle from hot-spot for inertial confinement fusion,” *Phys. Plasmas* **26**, 122701 (2019).
- ¹⁰⁸K. Li and W. Y. Huo, “Nonlocal electron heat transport under the non-Maxwellian distribution function,” *Phys. Plasmas* **27**, 062705 (2020).
- ¹⁰⁹F. García-Rubio, R. Betti, J. Sanz, and H. Aluie, “Self-consistent theory of the Darrieus–Landau and Rayleigh–Taylor instabilities with self-generated magnetic fields,” *Phys. Plasmas* **27**, 112715 (2020).
- ¹¹⁰J. Nilsen, A. L. Kritcher, M. E. Martin, R. E. Tipton, H. D. Whitley, D. C. Swift *et al.*, “Understanding the effects of radiative preheat and self-emission from shock heating on equation of state measurement at 100s of Mbar using spherically converging shock waves in a NIF hohlraum,” *Matter Radiat. Extremes* **5**, 018401 (2020).
- ¹¹¹Y. Gao, Y. Cui, L. Ji, D. Rao, X. Zhao, F. Li, D. Liu, W. Feng, L. Xia, J. Liu *et al.*, “Development of low-coherence high-power laser drivers for inertial confinement fusion,” *Matter Radiat. Extremes* **5**, 065201 (2020).
- ¹¹²R. K. Follett, J. G. Shaw, J. F. Myatt, H. Wen, D. H. Froula, and J. P. Palastro, “Thresholds of absolute two-plasmon-decay and stimulated Raman scattering instabilities driven by multiple broadband lasers,” *Phys. Plasmas* **28**, 032103 (2021).
- ¹¹³H. H. Ma, X. F. Li, S. M. Weng, S. H. Yew, S. Kawata, P. Gibbon, Z. M. Sheng, and J. Zhang, “Mitigating parametric instabilities in plasmas by sun-light lasers,” *Matter Radiat. Extremes* **6**, 055902 (2021).